CCS Chemistry

RESEARCH ARTICLE

Received: Aug. 3, 2020 | Accepted: Oct. 15, 2020 | Published: Nov. 17, 2020

DNA Nanotechnology for Modulating the Growth and Development of Neurons

Mirza Muhammad Faran Ashraf Baig[1], Chunxia Wen[2], Jian Li[1], Xiang Qin[1], Saud Asif Ahmed[1] & Xing-Hua Xia[1]*

[1]*State Key Laboratory of Analytical Chemistry for Life Science, School of Chemistry and Chemical Engineering, Nanjing University, Nanjing 210023,* [2]*Medical School, Nanjing University, Nanjing 210093*

**Corresponding author: xhxia@nju.edu.cn*

Cite this: *CCS Chem*. **2020**, *2*, 2381–2393

Late prenatal growth, early postnatal growth, and layering of the neocortical neurons (NC-Ns) play determining roles in the development of the cerebral cortex (CC). Here, we systematically explore the interactive role of neuronal surface receptors (NSRs) on cytoskeleton activation (CA) and the piconewton (pN) force generation (P-FG) and their influence on the proper development, growth, and functioning of neurons using a designed DNA nanomechanical device (DNA-NMD). This DNA-NMD, functioning as a molecular tension probe (MTP), can be used to selectively bind the different NSRs (β-NGFR, Reelin, and Integrin) to mono-, bi-, and trispecifically activate the receptors on the NC-Ns surface for imaging and calculating the P-FG involved in various processes. Measurements in vivo on the brain of newly born Institute of Cancer Research mice (early postnatal) or in vitro after extracting neurons from the fetal brain of pregnant Institute of Cancer Research mice (late prenatal) reveal that there are augmented interactive roles of the β-NGFR with Integrin and Reelin receptors (RR) on the CA and P-FG, resulting in enhanced directional migration of the neuronal endings (M-NEs), layering, and the somal terminal translocation (S-TT) followed by early postnatal growth.

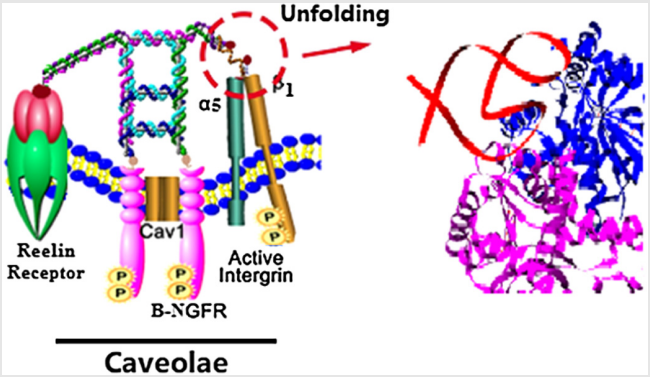

Keywords: neocortical neurons, neuronal surface receptors, migration of the neuronal endings, somal terminal translocation, DNA nanomechanical device, trispecific activation/deactivation

Introduction

Neuronal cells follow definite growth patterns during the developmental stage which make them different from other cells.[1] The unique patterned growth of neurons is guided by biochemical/mechanical signaling as a result of simultaneous activation of the neuronal surface receptors (NSRs) that give rise to enhanced cytoskeletal activations (CA) and piconewton (pN) force generation (P-FG).[1,2] A few reports suggest that the biochemical/mechanical interactions among different NSRs (Reelin and Integrin) are necessary for the neurons to undergo directional growth, growth cone pruning, pathfinding, and development into definite patterns.[3] The cerebral

DOI: 10.31635/ccschem.020.202000456
Citation: *CCS Chem*. **2020**, 2, 2381–2393
Citation denotes calendar and volume year of first online publication.
Issue Assignment: Volume 3 (2021), Issue 9

cortex (CC), the largest part of the brain, is an outer-layered structure involved in sensation, voluntary response, reasoning, and memory.[4] The development process of the neocortical neurons (NC-Ns) (from late prenatal to early postnatal and late postnatal stages) into mature CC (M-CC) follows highly complex growth patterns.[5] However, there is an incomplete explanation of the specific functions of the individual receptors, the interactions between different NSRs, and the involved P-FG and their impacts on subsequent stages of growth and development processes of the NC-Ns developing into M-CC.[6] Hence, it is crucial to comprehensively understand the physical and biomechanical roles of individual NSRs and interactions between different NSRs (β-NGFR, Reelin, and Integrin).[5,7] We find that monospecific activations of individual receptors have distinct effects on the growth and development pattern of the neurons. The trispecific simultaneous activations of the NSRs causes overlapping signal transduction pathways, which further activate the accessory NSRs (caveolin-1 and N-cadherin) (Figure 1) to coparticipate in enhancing the CA, P-FG, neuronal surface adhesion, growth, pathfinding, and development processes. This activation enables us to understand of NC-Ns conversion into M-CC better.[8]

After complete maturation, a properly functioning mammalian CC consists of six layers from inner ventricular zone (VZ) to the outer marginal zone (MZ).[9,10] The brain of a new born mammal lacks the well-developed CC called the neocortex (NC).[9]However, during the late fetal stage and immediately after the birth, the NC-Ns start to align through the layers from the VZ in an outside direction toward the MZ as an important step to be converted into M-CC.[9] Thus, the newly developed layers of neurons appear in an directional manner toward the surface.[11] This directional migration of neurons occurs due to the P-FG, which is caused by the Integrin-mediated cytoskeletal activation and its interactions with other NSRs (β-NGFR and Reelin) to augment P-FG and adhesion to the radial glial fibers (RGFs). According to our findings, the shear stress is enhanced to the extrathreshold level by trispecific activations of the receptors, which more efficiently facilitates the migration of the neuronal endings (M-NEs)

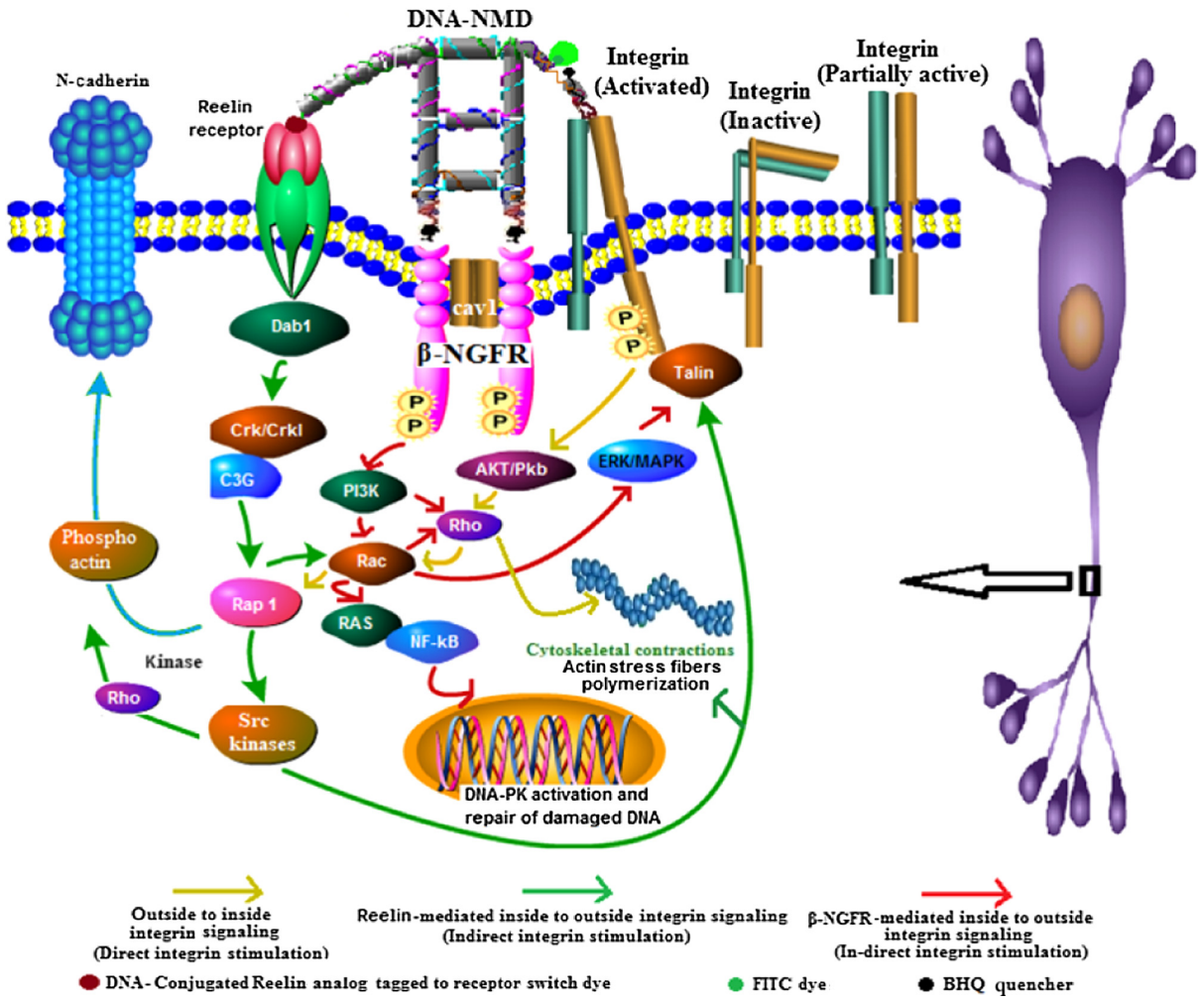

Figure 1. | *Mechanism of trispecific activation of NSRs. DNA-NMD interacts mono-, bi-, or trispecifically with the intended NSRs after programmed functionalization with the ligands or inhibitors.*

DOI: 10.31635/ccschem.020.202000456
Citation: *CCS Chem.* **2020**, 2, 2381–2393
Citation denotes calendar and volume year of first online publication.
Issue Assignment: Volume 3 (2021), Issue 9

outward followed by the improved somal terminal translocations (S-TT) and late postnatal growth.[12]

Past decades have witnessed the use of DNA-based nanodevices for mono- or bispecific activations on cell surfaces for bioimaging, drug delivery, and biosensing.[13–15] Here, we design a unique DNA nanomechanical device (DNA-NMD) for trispecific activation/deactivation of NSRs (β-NGFR, Reelin, and Integrin) to understand the signal transduction pathways as illustrated in Figure 1 and to image the growth and development processes of the NC-Ns.[16] A circular DNA scaffold with a specific length and sequence along with various staple strands after ligation and functionalization steps (Supporting Information Figure S1) has been used to synthesize DNA-NMD.[17,18] The sequences of various oligonucleotides used are given in Supporting Information Tables S1–S3. While the characterization experiments for DNA-NMD have been shown in Supporting Information Figure S2–S7. The rigid rectangular core made of circular scaffolding tremendously increases the mechanical strength of DNA-NMD to image the biophysical events for the calculation of involved P-FG and interactions between NSRs.[19]

Simultaneous trispecific activations of NSRs

The designed DNA-NMD, in comparison with the mono- or bispecific action of the NSRs, after functionalizing with various receptor activators/deactivators, enables us to

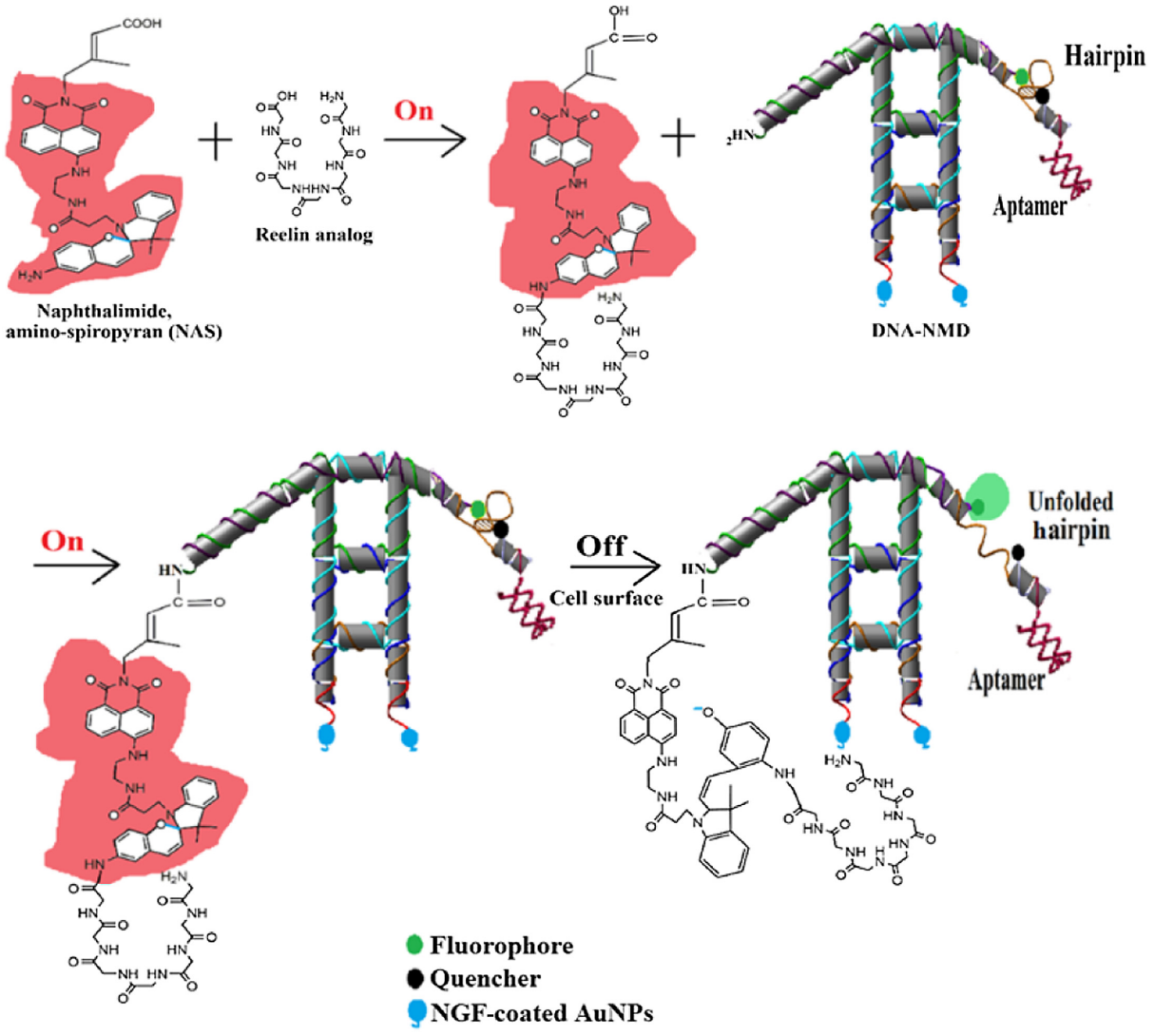

Figure 2. | *Scheme illustrating the "On–On–Off" function of the NAS probe attached at the left arm of DNA-NMD to confirm trispecific binding of DNA-NMD to NSRs. Red fluorescence of the NAS probe on the left arm of DNA-NMD turns off after its attachment to the neuronal surface due to the configuration inversion followed by amide bond breakage (weaker bond).[24] Thus, only green fluorescence is observed due to the unfolding of the hairpin structure on the right arm of DNA-NMD after binding with NSRs.*

DOI: 10.31635/ccschem.020.202000456
Citation: *CCS Chem.* **2020**, 2, 2381–2393
Citation denotes calendar and volume year of first online publication.
Issue Assignment: Volume 3 (2021), Issue 9

comprehensively understand the roles of individual receptors in the development of the brain.[2] The activation of one receptor may trigger activation of another receptor through intracellular signaling pathways (Figure 1).[20] Our DNA-NMD functionalized with various analogs/inhibitors enables us to fully manipulate activations/deactivations of the NSRs simultaneously to monitor the effects of the specific activations of interest related to neuronal growth, while inhibiting the irrelevant activations.[21] For the simultaneous trispecific activation of β-NGFR, Reelin and Integrin, the anchor strands of DNA-NMD are functionalized with the β-NGF-coated gold nanoparticles (AuNPs) (2 nm diameter) to bind/activate the β-NGFR dimers in the caveolae of the neuronal surface.[22,23] Meanwhile the left arm of the device is functionalized with Reelin analog to interact with the Reelin receptors (RR). Interaction of the left arm of the DNA-NMD with the RR causes conformational inversion followed by the amide bond breakage (weaker bond) of the naphthalimide amino-spiropyran (NAS) probe (receptor On/Off dye), which turns off the red fluorescence as shown by the scheme in Figure 2 and results in Supporting Information Figure S7.[24]

The right arm of the DNA-NMD is designed to contain either the Integrin binding aptamer (Aptamer 1 in Supporting Information Table S3) or the RGD (Arg-Gly-Asp, tripeptides consisting of Arginine, Glycine, and Aspartate) peptide (or fibronectin) to attach and activate the Integrin.[25] To inhibit the Integrin receptors, fibronectin-CS1 (FN-CS1) is attached to the right arm of the DNA-NMD that binds with Integrin; however, it cannot activate Integrin since FN-CS1 does not include the RGD portion. The right arm of DNA-NMD containing a hairpin structure can be used to sense the pN forces caused by Integrin activation via unfolding of the hairpin structure. The unfolding of the hairpin causes the fluorophore–quencher pair to separate, turning on the fluorescence signal.[26] The longer hairpin with more GC (Guanine-Cytosine pairing) content requires larger forces to unfold the hairpin. This generates intense fluorescence signals due to the greater distance between the fluorophore and the quencher.

Imaging was performed using traction force microscopy (TFM)[27] and molecular tension probe (MTP) on a laser confocal fluorescence microscope (MTP-LCFM)[28] to detect changes in P-FG during the growth of NEs, layering, S-TT, and early and late postnatal growth of CC neurons. Trispecific activation enables us to image the directional growth and realignment of the NC-Ns either in vivo or in vitro on a polyamide-functionalized surface (PA-F) acting as a simulated RGF. In this way, NEs of the NC-Ns migrate through the various layers toward the MZ (in vivo) or the poly-L-lysine (PLL) layer (in vitro) (poly-L-lysine acting as a simulated MZ). Ultimately, NC-Ns undergo the S-TT process involving the cell body (soma) moving toward the MZ (or PLL line) to exhibit S-TT.[11]

Experimental Methods

Synthesis of AuNPs

The AuNPs with 2 nm diameter were synthesized using $NaBH_4$ reduction method.[29] Heating the solution caused rapid reduction. We observed the change in the yellow color of $HAuCl_4$ solution to white, black, and ultimately to deep red. The synthesized AuNPs were characterized using UV–vis spectroscopy (Shimadzu UV1800, Kyoto, Japan), dynamic light scattering (DLS) instrument Zeta Plus 90 (Brookhaven Instruments Corporation, NY, USA), and transmission electron microscopy (TEM; JEM-JEOL1230, Tokyo, Japan).

AuNPs-functionalized DNA strands (AuNPs@DNA)

The DNA strands (red strands) intended to be attached to the AuNPs were modified at the 5′ end with the dithiol/ moiety, which acts as an elastic linker between the DNA strands and the AuNPs.[30] A 30 μL of 10 mM AuNPs (2 nm diameter) suspension was placed in a tube containing 1.85 mL of MilliQ ultrapure water to obtain a AuNPs suspension (15 nM). Then, 20 μL of 30 μM DNA oligonucleotide solution (with 5′ end modified with dithiol) was incubated with the above solution. After incubating for 20 min at room temperature, 30 μL of 10% sodium dodecyl sulfate (SDS) commercial solution [Sangon Biotech (Shanghai) Co., Ltd., Shanghai, China] was put into the above solution to make a final solution containing approximately 0.1% SDS. A 50 μL of 0.2 M phosphate buffer with pH 7.5 was put into the above solution to obtain 0.01 M phosphate. A 200 μL of 1 M NaCl solution was put into the above solution to obtain the final concentration containing approximately 0.1 M NaCl. The mixture was stirred for 25 min followed by the further addition of 200 μL of 1 M NaCl. The solution was stirred for another 25 min. The process of addition of NaCl was continued two or three more times until the final solution containing 0.3–0.4 M NaCl. The mixture was continued to be stirred for overnight to ensure complete attachment of the AuNPs to the DNA oligonucleotides. The synthesized AuNPs@DNA suspension was centrifuged at 15,000 rpm for 30 min at 4 °C followed by discarding the supernatants and resuspending the AuNPs@DNA in phosphate-buffered saline (PBS). The AuNPs@DNA was washed three times.

β-NGF coating over anchoring AuNPs of AuNPs@DNA (to function as the anchoring points on DNA-NMD structure for β-NGF/β-NGFR interaction)

A β-NGF coating on AuNPs of AuNPs@DNA was applied as mentioned by Song et al.,[22] with modifications. Briefly,

DOI: 10.31635/ccschem.020.202000456
Citation: *CCS Chem.* **2020**, 2, 2381–2393
Citation denotes calendar and volume year of first online publication.
Issue Assignment: Volume 3 (2021), Issue 9

the AuNPs@DNA solution (30 μM, μL) was incubated for 24 h with 0.30 mg/mL, 16-mercaptohexadecanoic acid (MHDA) (5 μL) at room temperature. After that 2 μL, 0.4 mM, *N*-ethyl-*N*-(3-dimethylaminopropyl)carbodiimide (EDC) solution was added and incubated for 60 min. This solution was finally incubated with 3 mg/mL β-NGF solution (5 μL) for 24 h at room temperature to get the β-NGF coating over AuNPs of AuNPs@DNAs. The AuNPs@DNAs with the β-NGF coating over its AuNPs were purified by centrifugation followed by the discard of the supernatants. This washing process was repeated three times. Finally, the β-NGF-coated AuNPs attached to the DNA were suspended in 50 μL 1% bovine serum albumin (BSA) and stored in the refrigerator. β-NGF-coated AuNPs on the AuNPs@DNAs (AuNPs-functionalized DNA oligos) underwent further annealing with the staple strands to make DNA-NMD that had anchoring ability onto the caveolae of neurons due to the β-NGF/β-NGFR interactions.

Synthesis of circular scaffolds

The 5′ phosphorylated linear strand (108-NT) was circularized with the help of splint strands as described previously.[17,31] Briefly, the 108-NT circular template was prepared by annealing (98–25 °C) the linear strand phosphorylated at its 5′ end (60 μM, 80 μL) with the splint strands (70 μM, 100 μL) gradually for 5 h.[32] Splint strands helped in bringing two ends of linear strands together. After that, a DNA ligase overnight treatment was applied at 16 °C in an ethanol bath. DNA ligase linked the two ends of linear strands together covalently. However, some strands remained uncircularized. Also, the splint strands were not circularized during this reaction. To digest and break all of the uncircularized strands, Exonuclease-1 treatment was applied. The circular template strand underwent purification by polyacrylamide gel electrophoresis (PAGE) (denaturing type having urea). Bands for the circular strand were cut to extract the entrapped scaffolds by maceration for 2–3 days using a tube-shaking device.

Synthesis of DNA-NMD

The 108-NT circular strand was prepared to act as a scaffold strand to attain firm rectangular core structure after annealing with the staple strands (66-NT, 60-NT, and 36-NT) from 95 °C to room temperature.[17] The functionalizing strands (18-NT; purple strand@fluorophore, 21-NT to 26-NT), brown hairpin strand (12-NT; white strand@quencher), and red aptamer strands were added stoichiometric wise with the final concentration of DNA-NMD to be 25 μM. This final mixture was annealed from 70 °C to room temperature to allow the self-assembly of the functionalizing strands to the core structure. Finally, all the nicks were joined together using T4-Ligase overnight at 16 °C followed by deactivation of DNA ligase by treating it at 65 °C for 10 min. The ligation process gives the DNA-NMD a stable and rigid conformation to carry out stress and force measurements.

Functionalization of the left arm of DNA-NMD

NAS/Reelin analog was attached to the left arm of the DNA-NMD.[33] It retained red fluorescence after attachment to the DNA-NMD. However, after attaching itself to the neuronal surface, it underwent configurational inversion and loss of fluorescence as illustrated in Figure 2.[24]

PAGE electrophoretic (stability and integrity testing of DNA-NMD)

The stability and integrity of the designed DNA-NMD were tested by running it through 10% PAGE.[34] After undergoing the ligation process, DNA-NMD was stable enough and gave one sharp band during electrophoresis. There was a slight difference in electrophoretic mobility between functionalized and unfunctionalized DNA-NMD due to the firm two-dimensional (2D) core and a slight difference in the configuration in either case.[35] It confirmed that design, shape, and configuration of the designed DNA-NMD were consistent with expectations.

Mechanism for the selective mono-, bi- and trispecific activations of receptors by DNA-NMD

The monoactivation of RRs was achieved by attaching the Reelin analog to the left arm of DNA-NMD and inhibiting the other two receptors by attaching blocking antibodies to DNA-NMD. β-NGFR was inhibited by functionalizing the anchor strands of DNA-NMD with the Au-NPs coated with anti-β-NGFR antibody that enables DNA-NMD to fix inside the caveolae after binding the β-NGFR (without activating it). Meanwhile the right arm of the DNA-NMD was functionalized with FN-CS1 (which lacks the RGD portion) that can bind with the Integrin without activating it.[36] Therefore, our DNA-NMD was designed for the programmed monospecific activation of RRs. The monospecific activation of β-NGFR was achieved by functionalization of the anchor strands with the β-NGF@AuNPs (β-NGF-analog-coated AuNPs) that enables DNA-NMD to interact and activate the β-NGFR and be fixed inside the caveolae. RRs were blocked by modifying the left arm with the anti-Reelin antibody that could bind with the RRs but block the receptors. Furthermore, the Integrin was inhibited through a right arm functionalized with the FN-CS1 as mentioned above. In this case, the Integrin was solely activated because of the indirect pathway mediated by the β-NGFR. The Integrin receptor underwent monospecific activation by blocking

DOI: 10.31635/ccschem.020.202000456
Citation: *CCS Chem.* **2020**, 2, 2381–2393
Citation denotes calendar and volume year of first online publication.
Issue Assignment: Volume 3 (2021), Issue 9

the other two receptors as mentioned earlier and functionalizing the right arm of the DNA-NMD with its complement aptamer or RGD protein[37] that shows strong binding affinity to the Integrin and activates it. By manipulating the aforementioned techniques, we were able to achieve mono-, bi-, and trispecific activations of the receptors and observe the effects on different neuronal processes.

Administration of DNA-NMD to fetal brain of the Institute of Cancer Research (ICR) mice for prenatal in vivo experiments

The fetus was removed from the mother by surgery at the prenatal stage on the 14th day of pregnancy. The brain is comparatively soft at this stage for the intrathecal administration of DNA-NMD (30 μL, 30 μM hourly injection) into the subarachnoid space to be distributed by the cerebrospinal fluid to the different layers of CC. The microscopic sections were prepared after 3 hours of administration of DNA-NMD to the fetal brain for prenatal study. Because the prenatal brain is not so much developed and does not have distinct differentiation between the individual layers, we could only show the overall pattern of arrangement of different layers in one image. The microscopic analysis of the brain section only showed the rough overall pattern of the arrangement of the neurons. Due to the larger area of focus comprising of different layers of neurons, each neuron appeared as a dot in the image.

Extraction of NC-Ns for culture

NC-Ns from the fetus of pregnant ICR mice were collected. The mating of the mice was followed by the use of vaginal plugs with the female mice. The duration of pregnancy was counted as day 1 of the embryo. The method adopted for the extraction of NC-Ns has previously been described.[5,38] Mice were cared for and underwent dissection according to the ethics and guidelines set by the Medical School of Nanjing University (Nanjing, China).

Preservation of the freshly removed brain sections

Fetal brain sections of the NC from the pregnant mice were quickly put into the PBS solution (ice cold). Optimal cutting temperature compound was used to embed these neocortical sections prior to being frozen in a liquid nitrogen tank. These cryopreserved sections served as a continuous source of the neurons during the study of NC-Ns.[39]

Preparation of the single-neuron suspension

To obtain single-neuron suspensions, the neocortical brain sections of embryonic mice were treated with the 0.8% Trypsin-ethylenediaminetetraacetic acid (EDTA) under 5% CO_2 at 37 °C for 20 min. Fresh prewarmed Dulbecco's modified Eagle's medium (DMEM) with 10% Fetal Bovine Serum (FBS) was used to deactivate the trypsin, and a 5 mL pipette was used for crushing and triturating the trypsinized neocortical sections into the single-neuron suspension. The cell count was maintained at 70,000 cells/mL. Freshly extracted neurons were centrifuged and suspended back in the fresh culture medium.[38]

Neurons with migrating potential

The NC-Ns selected for the experiments were from different depths and regions of the neocortical sections. After initial experiments and confirmation, we decided to collect the neurons from the somatosensory part of the NC. However, as migrating cells were present deep beneath the marginal cortical plate (CP) and intermediate zoon (IZ), we used the neurons extracted from different depths of the neocortical brain sections blindly, estimating the migratory potential by activating different receptors using our DNA-NMD on PA-F surfaces. Each experiment was repeated at least three times to ensure that results were statistically significant ($p \leq 0.05$).[39]

In vitro study of the migratory NC-Ns to monitor S-TT process

Simulating the conditions of the three-dimensional (3D) fibrous extra-cellular matrix (ECM) environment in vitro to that of the brain (presence of glial fibers) was achieved by growing the NC-Ns on the PA-F surfaces. A PLL line was applied to the functionalized coverslip. The neuronal growth adhered at a certain distance from the PLL line (100–120 μm distance) and was monitored from the zone of initial adhesion. These neurons were evaluated for the growth of the neurites toward the PLL line. After activating different receptors on the neuronal surface by our DNA-NMD, the motion of the migrating neurites was monitored for 3 h. Neurons with effective activation of receptors might be able to generate sufficient cytoskeleton activity and M-NEs to reach the PLL line. Since the PLL line was positively charged, it acted as a simulator layer to that of the MZ in the brain. M-NEs might be able to adhere to this layer and might involve indirect N-cadherin receptor activation via RR and undergo the S-TT process. Molecular probe fluorescence microscopy and TFM equipped with 40× objectives were used to estimate the pN forces generated and the shear stress that cause neurons to grow toward the PLL line. The Z range and Z focus were acquired using SP5 (Leica microsystems, NC, USA).[5]

Treatment of NC-Ns to the DNA-NMD

A glass coverslip was coated with Poly-acryl-amide (PAA) functionalized (PA-F) surfaces. A PLL line was applied at different points along the coverslip with

DOI: 10.31635/ccschem.020.202000456
Citation: *CCS Chem.* **2020**, 2, 2381–2393
Citation denotes calendar and volume year of first online publication.
Issue Assignment: Volume 3 (2021), Issue 9

spacing of 0.05 mm using a specially designed applicator. The functionalized coverslip was placed in the petri dish. A 5 mL neuronal cell suspension in high glucose DMEM containing 10% FBS purchased from Sangon Biotech (Shanghai) Co., Ltd. was added to the petri dish. Neurons were incubated in 5% CO_2 at 37 °C for 1 h to allow the initial adhesion of the neurons to the PAF surface. After that 500 μL, 50 μM DNA-NMD solution was added. Due to the ligands attached to the DNA-NMD, it activated certain receptors on the neuronal surface. The DNA-NMD dose was repeated every 30 min due to its internalization into neurons as well as the photobleaching effect, thereby maintaining continuous activation of the receptors and the fluorescence signals.

DNA-NMD binding assay to activate NSRs

After being dissociated into single neuronal suspensions, the excised embryonic cortical brain sections were made to adhere onto the PAF surface as mentioned earlier. After initial adhesion of the neurons to this surface, DNA-NMD (50 μM, 500 μL) was added. Neurons were incubated with 5% CO_2 at 37 °C for 1 h. Then the media were removed, and cells were washed three times with the prewarmed PBS. The coverslip was removed from the petri dish and put on the glass slide for confocal examination of fluorescent color. As DNA-NMD was equipped with the β-NGF-coated AuNPs on its anchor strands, it was stabilized on the caveolae of neurons due to the β-NGF/β-NGFR interactions. After binding to the RR, the left arm of the DNA-NMD underwent configurational inversion that resulted in the loss of fluorescence (switch off) of the naphthalimide amino-spiropyran (NAS) probe.[24] The right arm of DNA-NMD equipped with the hairpin structure was made to attach and activate the Integrin receptors. Integrin activation was confirmed by the force exertion onto the hairpin structure of DNA-NMD as evidenced by the unfolding and generation of green fluorescence signals due to the separation of the FITC (Fluorescein isothiocyanate; fluorophore) and the BHQ2 (Black-Hole Quencher 2; quencher).[26]

Western blotting

After being seeded in the six-well plates, neurons underwent starving using a medium with 0.5% BSA for one more day. Different antibodies [Sangon Biotech (Shanghai) Co., Ltd.] were evaluated for their binding efficiency with the substrates by incubating the antibodies with the respective substrates under the prescribed buffer following the company's user manual. DNA-NMD 50 μL, 25 μM solution was added to the cells followed by the incubation for 30 min. We used a Radioimmuno-precipitation assay (RIPA) lysing/buffer for cell lysing after PBS washing. This was supplemented with protease phosphatase inhibitors to keep the polymerized and phosphorylated proteins in the cell lysates intact for analysis. Centrifugation was performed at 10,000*g* for about 25 min to recover the supernatants. After estimating the concentrations, proteins were loaded to the 15% SDS PAGE followed by the transfer of the bands to the polyvinylidene difluoride (PVDF) membranes. About 5% milk/Tris-buffered saline + 0.1% Tween 20 (TBST) was used to block the nonspecific interactions for 1–2 h. The fluorescent-labeled primary antibodies for Ph-integrinβ4, Ph-NGFR, Ph-Erk1,2, ph-Akt, and so forth were incubated for 1 h at room temperature or 6–8 h in the refrigerator. TBST washing was followed by treatment with the labeled secondary antibodies with Alexa Fluor dye for about 60 min at 25 °C. Washing was performed again three times using TBST, followed by the analysis of the bands using SuperSignal West Pico chime-luminescent-analysis/apparatus and the gel-analyzing instrument.

Unfolding of hairpin and P-FG calculations

The unfolding of the hairpin portion of DNA-NMD was induced by the force generated after activating the Integrin molecule on DNA-NMD attached to the neuronal surface. The algorithms were devised based on unfolding upon Integrin activation. This unfolding experiment followed a first-order kinetic rate as illustrated by eqs 1 and 2 below, and according to Markov phenomenon as reported.[28,40]

$$C_U(f) = C_o \exp\left(-\frac{B.f}{C_B.T}\right) \quad (1)$$

$$C_F(f) = C_o \exp\left(-\frac{B.f - dG_{F\to U}(f)}{C_B.T}\right) \quad (2)$$

C_U and C_F are the coefficients for the unfolding/folding states under applied force f, C_o is the diffusive attempt frequency (DAF) coefficient, and $dG_{F\to U}(f)$ is the difference of fully folded/unfolded states under the applied force (f).

The hairpin with partially opened (n) to fully opened (N) states at base pair levels were calculated by the worm-like chain (WLC) model and the nearest-neighbor (NN) model for single/DNA-NMD unfolding using the following eq 3.[40]

$$dG_{Fn}.f = \nu(-\sum_{i}^{n} I.gi,i+I-g_{I\partial_{nN}}) + dg_{Fn}^{ssDNA}.f + dg_{Fn}^{d}.f \quad (3)$$

where $(-\sum_{i}^{n} I.gi,i+I-g_{I\partial_{nN}})$ represents the dG^{o}_{FN} as the unfolding of a hairpin on DNA-NMD due to the applied force f, While dg_{Fn}^{ssDNA} is the unfolded elastic state of single-stranded DNA (ssDNA). ν is the variance for noise. The pixel threshold algorithm was designed and neighborhood was kept to be 2 × 2 pixels. We wrote a MATLAB script to convert pixels into quantitative data about neuronal spreading and morphological variability upon cytoskeletal activation. The script traced the neuronal trajectories,[41] by observing the fluorescent images after the addition of 5–10 μM DNA-NMD solution into 10^1–10^2 neurons.

DOI: 10.31635/ccschem.020.202000456
Citation: *CCS Chem.* **2020**, 2, 2381–2393
Citation denotes calendar and volume year of first online publication.
Issue Assignment: Volume 3 (2021), Issue 9

The neuronal surface density of β-NGFR/Integrin/Reelin to interact with DNA-NMD and variation of pixels to measure force per unit area on neurons

Force per area of cells on the neuronal surface was dependent on the fluorescence changes. It relied on the density of DNA-NMD bound to the β-NGFR/Integrin/Reelin on the neuronal surface with the unfolding of hairpin on the right side arm due to Integrin activation giving a certain amount of pixel intensity.[42] From the variations of pixel, force measurements were performed, and the minimum force measured was regarded as the unfolding F1/2 (unit quantity). The multiplying method was employed to calculate the total force on the neuronal surface. The experiments demonstrated the linear relationship between the fluorescence changes with the force on the surface of neurons. According to the fluorescence imaging, it was found that the neuronal surface was saturated by DNA-NMD, indicating the presence of a high density of β-NGFR/Integrin/RR.

Animal studies

We strictly followed the guidelines for the ethical treatment of laboratory animals during all the experiments involving the ICR mouse model, as set forth by the Chinese Ministry of Health and the Medical School of Nanjing University.

Statistical analysis

The nonnormally distributed data were evaluated statistically by undergoing nonparametric analysis. After the background noise was removed, the designed coding in the MATLAB program along with the special imaging tools was used to exclude the noise signals. Then the images as well as the stress calculation from the changes in pixels were processed.[27,42] We repeated each type of experiment at least three times to get an averaged pattern of measurements. The neurons that did not show cytoskeletal spreading and failed to adhere were rare and were excluded from the measurements. Experiments about the growth of neurons were repeated from 3 to 10 times to ensure repeatable results with statistically significant ($p \leq 0.05$). Force (pN) and shear stress (kPa) measurements were selected randomly among individual experiments. Direct comparisons ($n \leq 10$) were performed using the Mann–Whitney U test. Meanwhile the multiple parameters were assessed through analysis of variance (ANOVA), along with Tukey's posthoc test with the measurements of standard errors shown in the bar graph in Supporting Information Figure S8.

Results and Discussion

Imaging the development process of the NC-Ns using DNA-NMD

The difference between the fully developed CC and the NC is shown in Figure 3a. In the in vivo experiments, we observed the effects of different combinations of the bi- or trispecific activations/deactivations of NSRs on the neuronal development of CC to understand the conversion from NC to mature cortex.[5,16] We found that simultaneous bispecific activations of NSRs with different combinations (while the third receptors is inhibited simultaneously) show different effects on the layering process during brain development (Figures 3b–3d and Supporting Information Figures S9a–S9c).[43] As layering is a quite complex process involving a series of events, we tried to understand the augmented roles of three different NSRs in late prenatal NC neurons of the brain of ICR mice (Figure 3e and Supporting Information Figure S9d). The in vivo imaging of the layering process from the undifferentiated germ cells in the areas near the ventricular (VZ) and subventricular zones (SZ) toward the MZ with the possibility of S-TT process[5] under the generated stress and CA due to the activation of NSRs (β-NGFR, Reelin, and Integrin) are shown in Figure 3.[4] As the hairpin on the right arm of DNA-NMD is functionalized with a fluorophore–quencher, CA, P-FG, and shear stress caused by the activation of NSRs, and subsequent CA/P-FG will unfold the DNA hairpin structure to generate fluorescence signals. The longer hairpin with more GC contents requires larger forces to unfold the hairpin, which generates intense fluorescence signals due to the longer distance between the fluorophore–quencher (upon unfolding) and vice versa.[44] Hence, more force is required to unfold the longer hairpin, especially with increased GC (triple hydrogen-bond base pairing) contents than adenine-thymine (AT) (double hydrogen-bond base pairing) contents. In vivo experiments were performed on the early postnatal brain of newly born ICR mice, while in vitro experiments (discussed later) were carried out on the extracted neurons of the late prenatal brain from the fetus of the pregnant ICR mice.[38] The patterns of the growth after activation of different receptors (either one by one or simultaneously) and the different parameters during the growth and development of the late prenatal neurons (in vitro), early postnatal (in vivo), and late postnatal neurons (in vitro) have been explained in the Supporting Information in respective sections. However, a generalized pattern of the effects of activation of different NSRs has been summarized in Supporting Information Figure S8.

In vivo experiments to understand the growth and development of CC

As validated by the results from the histological experiment (Supporting Information Figure S9), western blot experiments (Supporting Information Figures S10 and S11 and Videos S1–S7) and in vitro experiments (discussed later) (Supporting Information Figures S12–S14, and Videos S1–S7), the outcomes of neuronal growth and development are improved after bi- or trispecific

DOI: 10.31635/ccschem.020.202000456
Citation: *CCS Chem.* **2020**, 2, 2381–2393
Citation denotes calendar and volume year of first online publication.
Issue Assignment: Volume 3 (2021), Issue 9

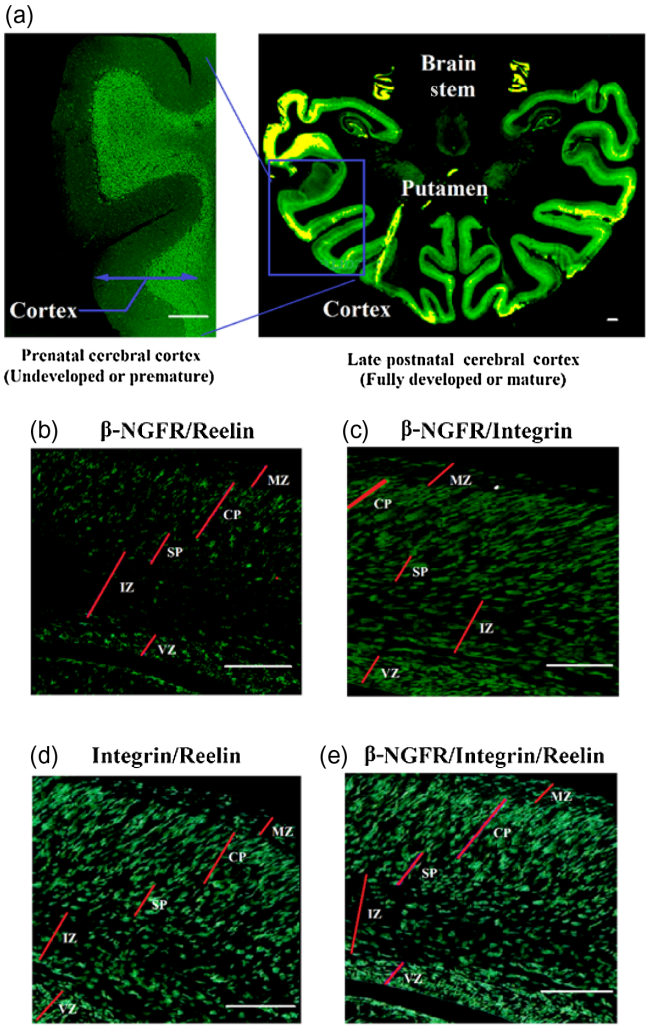

Figure 3. | *In vivo experiments showing the development process of the NC-Ns using DNA-NMD. (a) Differences between the prenatal (undeveloped) and late postnatal (fully mature) CC. (b) Improper layering of the neurons after bispecific activation of β-NGFR/Reelin (while inhibiting Integrin) showing weak P-FG (dim fluorescence) and increased adhesion. The neurons fail to show directional M-NEs to the level of MZ to exhibit S-TT. (c) Neuronal layering is slightly improved with a few neurons undergoing S-TT toward MZ after bispecific activation of β-NGFR/Integrin (while inhibiting RR), generating slightly improved pN forces (slightly intense fluorescence). (d) Neuronal layering is considerably improved with more neurons undergoing S-TT toward MZ after bispecific activation of Integrin/Reelin (while inhibiting β-NGFR receptors), generating improved pN forces (intense fluorescence) by unfolding the long DNA hairpins. (e) After trispecific activation, we can see the augmented role of β-NGFR/Integrin/RR as shown by the enhanced M-NEs and S-TT processes under the enhanced P-FG due to the unfolding of the longer hairpins (highly intense fluorescence). The scale bar of 1000 μm is the same for all images.*

activations of NSRs simultaneously as compared with the monospecific activation of individual receptors. Therefore, in our in vivo experiments (Figures 3b–3e and Supporting Information Figures S9a–S9d), we focused on bi- or trispecific activations of NSRs. After selective activations of the β-NGFR/Reelin (while inhibiting Integrin), we find that neurons are able to unfold short hairpins (16-NT length) with weak fluorescence signals, and they are unable to show considerable M-NEs toward IZ, although a few neurons display translocation to IZ as shown in Figure 3b.[45] The western blot experiments to estimate protein expression (Supporting Information Figures S10 and S11) show weak signal transduction in terms of low protein expressions, especially for Rho-kinase and F-actin. While the in vitro experiments about the growth of neurons shown in Supporting Information Figure S13a(i) and Video S4 further confirm that after selective β-NGFR/Reelin coactivations, the length of neurons is decreased due to the weak P-FG and shear stress. However, β-NGFR/Reelin coactivation

DOI: 10.31635/ccschem.020.202000456
Citation: *CCS Chem.* **2020**, 2, 2381–2393
Citation denotes calendar and volume year of first online publication.
Issue Assignment: Volume 3 (2021), Issue 9

can generate additional CA and P-FG than the individual receptors as both of these receptors cause weak and indirect Integrin stimulation (**inside to outside**) through different intracellular signal transduction pathways (Figure 1 and Supporting Information Videos S1–S4). In addition, expression of F-actin and Rho-kinase as indicators of CA increases in case of individual Reelin activation than β-NGFR (Supporting Information Figures S10 and S11). Nonetheless, the fact that the weak CA and P-FG, adhesion of the neurons to the PA-F surface is significant, as evidenced by the elevated Src-kinase[46] and N-cadherin expressions illustrated in the western blot experiments (Supporting Information Figure S10). Thus, the width of neurites and the area of the cell body show an increase, and the area of M-NEs shows a decrease (Supporting Information Figure S8).

After β-NGFR/Integrin bispecific activation (while inhibiting RR), the neurons are able to unfold longer hairpins (22-nt length), generating more intense fluorescence and many of the neurons crossing the IZ toward the CP.[16] However, only a few neurons exhibit straight growth and reach the MZ to exhibit S-TT (Figure 3c and Supporting Information Figure S9).[43] The increased M-NEs are due to the elevated P-FG (10–11.5 pN) resulting from the direct (**outside to inside**) Integrin activation that is enhanced with the coactivation of β-NGFR [Supporting Information Figure S13a(ii)].[7] The β-NGFR alone causes weak and indirect Integrin activation (**inside to outside**) through the intracellular signal transduction pathways than the direct Integrin activation (**outside to inside**) (Supporting Information Figure S11).[47] Hence, the M-NEs process is enhanced after β-NGFR/Integrin bispecific activation as compared with the activations of individual receptors [Figure 3c and Supporting Information Figure S13a(ii)] as evidenced by the elevated F-actin and Rho-kinase expression (Supporting Information Figure S11).[5] Therefore, selective β-NGFR/Integrin activation can cause augmented CA, P-FG and generation of shear stress (Supporting Information Figures S13b and S13c). However, this bispecific activation leads to the undirectional M-NEs (bent growth) and abnormal layering of NC-N, resulting from the weak/mild activation of N-cadherin due to the RR inhibition (Dab1-Src kinase pathway) (Supporting Information Figures S10 and S11).[46] We observe the appearance of the multipolar neuronal accumulation zone on the VZ and SZ layers toward the IZ with only a fraction of the neurons undergoing directional M-NEs to the level of MZ, exhibiting S-TT as shown in Figure 3c and Supporting Information Figure S9b.[46] These results are further confirmed by the results of in vitro experiments as shown in Supporting Information Figure S13a(ii) and Video S5, which reveal that bispecific activation of β-NGFR/Integrin considerably increases the length of neurons, while the growth of neurons becomes nonlinear (bent), and the adhesion, width of neurites, and the area of the cell body are decreased.[48] The process of M-NEs is further improved after bispecific activation of the Reelin/Integrin receptors (while inhibiting β-NGFR) due to direct (**outside to inside**) Integrin activation and larger P-FG as further confirmed by our in vitro experiments (Supporting Information Figure S14).[5] These receptor-specific effects were also explored for the development of the postnatal neurons (Supporting Information Figure S15).

In vitro trispecific activation of the RR/Integrin/β-NGFR

Tri-specific activation of RR/Integrin/β-NGFR in vitro achieves synergistically enhanced S-TT process as illustrated in Figure 4 and Supporting Information Video S7. There is a synergistic increase in the directional M-NEs and directional M-NEs straightly toward the PLL line. Neurons are able to unfold quite longer hairpins (up to 28-NT) resulting in extremely sharp fluorescence signals due to the complete separation between the fluorophore and the quencher.[26] Neurons experience enhanced CA and P-FG (≤15 pN), simultaneously showing a synergistic increase in the mechanical processes after the trispecific activation of the receptors (Figure 4b).[49] The overall length of neurons (≥110 μm) and the length of the neurites (30–75 μm) are significantly increased (Supporting Information Figure S8). The adhesion of the middle part of the neurons to the PA-F surface is considerable (≤50%). While the adhesion of the terminal part (≤98%) is significantly increased to guide the neurons to exhibit directional growth.[50] However, the thickness of the neurons (≤4 μm) and the area of the cell body (≤200 μm^2) as well as M-NEs (≤185 μm^2) are decreased as compared with the bispecific activation of RR/Integrin. As the monoactivation of RR has a triple role, including N-cadherin activation (Dab-1/Src-kinase-mediated),[43] direct actin-stress fibers activation (Dab-1/Rap-1mediated),[11] and indirect activation of Integrin (paxillin mediated),[45] it causes synergistically enhanced CA when β-NGFR activation is also involved[7] owing to the simultaneous indirect (**inside to outside**) + direct (**outside to inside**) activation of Integrin.[11,51] This trispecific activation not only gives rise to actin stress-fiber activation,[52] but also generates a threshold to involve the myosin-II stress-fibers,[53] enhanced CA, and P-FG. This leads the neurons to undergo the M-NEs and S-TT processes (up to 75% of the total neurons) more quickly (within 2–2.5 h) (Figures 4a–4c).[5] Hence, the directional growth of the neurons is considerably improved (straighter direction) toward the positively charged PLL line and generates stronger P-FG upon establishing the adhesion complex (with the PLL line).[38] This adhesion complex causes termination of the further increase in the length of the neurons, stopping the propagation of the MN-Es. Meanwhile, due to the significantly enhanced CA, the P-FG becomes reinforced due to the involvement of F-actin[6]

DOI: 10.31635/ccschem.020.202000456
Citation: *CCS Chem.* **2020**, 2, 2381–2393
Citation denotes calendar and volume year of first online publication.
Issue Assignment: Volume 3 (2021), Issue 9

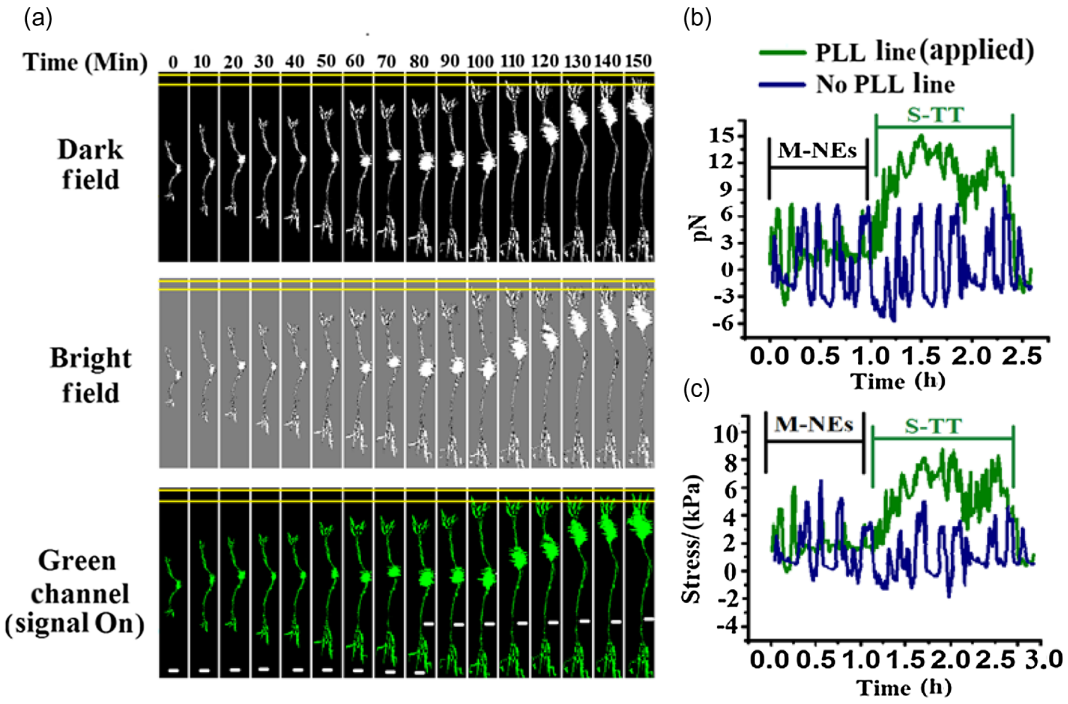

Figure 4. | *Effects of trispecific activation of RR/Integrin/β-NGFR on the growth and development of neurons (referred to Supporting Information Video S7). (a) Trispecific activation increases longitudinal growth with a slight decrease in the lateral growth of neurites and thickness. More cytoskeletal contractions are observed as evidenced by the periodic changes on the surface morphology of the cell body with enhanced directional growth toward PLL line undergoing S-TT process after 1.5 h when growing M-NEs adhere to the PLL line owing to the N-cadherin involvement. (b and c) Trispecific activation causes enhanced directional growth and synergistic increase in P-FG and shear stress especially after growing M-NEs adhered to the PLL line that causes initiation of the S-TT process after 1 h compared with the control (n = 12 cells, t test, ***p value < 0.005).*

and myosin-II stress fibers,[54] causing the neurons to experience more shear stress throughout their length toward the adhered MN-Es, which initiates the movement of the cell body (soma) toward the fixed NEs on the PLL line more quickly than that of bispecific activation of RR/Integrin.

Conclusion

We have designed a DNA-NMD to monitor and image the effects of mono-, bi-, and trispecific activations of NSRs (Integrin-α5β1, Reelin, and β-NGFR) on the different neuronal processes such as M-NEs, S-TT, early and late postnatal growth. We find that each receptor has its specific function in the development of brain. Integrin not only increases CA and P-FG but also has a role in increasing the length of neurites. RR further enhances CA, P-FG along with N-cadherin activation causing increased adhesion, pathfinding, and directional M-NEs. Additionally, β-NGFR involvement further enhances the CA, P-FG, and N-cadherin activity to support directional M-NEs, growth, and developmental processes of NC-Ns. Coactivations of NSRs results in synergistic functions of the receptors. For instance, trispecific activation leads to the synergistically enhanced S-TT process. The present DNA-NMD enables us to investigate the effects of individual receptors and image the interactions between the receptors through simultaneous activations/deactivations to comprehensively understand and manipulate the development processes of the brain, which might be helpful to design strategies to diagnose and combat neuro-degenerative diseases.

Supporting Information

Supporting Information is available.

Conflict of Interest

The authors declare no conflict of financial interest.

Funding Information

This work is supported by grants from the National Key R&D Program of China (no. 2017YFA0700500), the National Natural Science Foundation of China

(no. 21635004), and the Excellent Research Program of Nanjing University (no. ZYJH004).

Acknowledgments

Special thanks to the Medical School of Nanjing University for continuously providing the neurons for this study.

References

1. Alcántara, S.; Pozas, E.; Ibañez, C. F.; Soriano, E. BDNF-Modulated Spatial Organization of Cajal-Retzius and GABAergic Neurons in the Marginal Zone Plays a Role in the Development of Cortical Organization. *Cereb. Cortex* **2006**, *16*, 487–499.
2. Zhang, Y.; Moheban, D. B.; Conway, B. R.; Bhattacharyya, A.; Segal, R. A. Cell Surface Trk Receptors Mediate NGF-Induced Survival While Internalized Receptors Regulate NGF-Induced Differentiation. *J. Neurosci.* **2018**, *20*, 5671–5678.
3. Wang, Y.; Shan, Q.; Pan, J.; Yi, S. Actin Cytoskeleton Affects Schwann Cell Migration and Peripheral Nerve Regeneration. *Front. Physiol.* **2018**, *9*, 23.
4. Alcántara, S.; Ruiz, M.; D'Arcangelo, G.; Ezan, F.; de Lecea, L.; Curran, T.; Sotelo, C.; Soriano, E. Regional and Cellular Patterns of Reelin MRNA Expression in the Forebrain of the Developing and Adult Mouse. *J. Neurosci.* **2018**, *18*, 7779–7799.
5. Sekine, K.; Kawauchi, T.; Kubo, K. I.; Honda, T.; Herz, J.; Hattori, M.; Kinashi, T.; Nakajima, K. Reelin Controls Neuronal Positioning by Promoting Cell-Matrix Adhesion via Inside-Out Activation of Integrin A5β1. *Neuron* **2012**, *76*, 353–369.
6. Harrington, A. W.; St. Hillaire, C.; Zweifel, L. S.; Glebova, N. O.; Philippidou, P.; Halegoua, S.; Ginty, D. D. Recruitment of Actin Modifiers to TrkA Endosomes Governs Retrograde NGF Signaling and Survival. *Cell* **2011**, *146*, 421–434.
7. Balzamino, B. O.; Esposito, G.; Marino, R.; Keller, F.; Micera, A. NGF Expression in Reelin-Deprived Retinal Cells: A Potential Neuroprotective Effect. *Neuromolecular Med.* **2015**, *17*, 314–325.
8. Qi, J.; Wang, J.; Romanyuk, O.; Siu, C. H. Involvement of Src Family Kinases in N-Cadherin Phosphorylation and β-Catenin Dissociation during Transendothelial Migration of Melanoma Cells. *Mol. Biol. Cell* **2006**, *17*, 1261–1272.
9. Ringstedt, T.; Linnarsson, S.; Wagner, J.; Lendahl, U.; Kokaia, Z.; Arenas, E.; Ernfors, P.; Ibáñez, C. F. BDNF Regulates Reelin Expression and Cajal-Retzius Cell Development in the Cerebral Cortex. *Neuron* **1998**, *21*, 305–315.
10. Ajioka, I. Biomaterial-Engineering and Neurobiological Approaches for Regenerating the Injured Cerebral Cortex. *Regen. Ther.* **2016**, *3*, 63–67.
11. Sekine, K.; Kubo, K. I.; Nakajima, K. How Does Reelin Control Neuronal Migration and Layer Formation in the Developing Mammalian Neocortex? *Neurosci. Res.* **2014**, *86*, 50–58.
12. Dingyu, W.; Fanjie, M.; Zhengzheng, D.; Baosheng, H.; Chao, Y.; Yi, P.; Huiwen, W.; Jun, G.; Gang, H. Regulation of Intracellular Structural Tension by Talin in the Axon Growth and Regeneration. *Mol. Neurobiol.* **2016**, *53*, 4582–4595.
13. Yue, S.; Song, X.; Song, W.; Bi, S. An Enzyme-Free Molecular Catalytic Device: Dynamically Self-Assembled DNA Dendrimers for in Situ Imaging of MicroRNAs in Live Cells. *Chem. Sci.* **2019**, *10*, 1651–1658.
14. Baig, M. M. F. A.; Zhang, Q.-W.; Younis, M. R.; Xia, X.-H. A DNA Nano-Device Simultaneously Activating the EGFR and Integrin for Enhancing Cytoskeletal Activity and Cancer Cell Treatment. *Nano Lett.* **2019**, *19*, 7503–7513.
15. Baig, M. M. F. A.; Abbas, M.; Naveed, M.; Kassim, S. A.; Khan, G. J.; Sohail, M.; Ullah, S.; Hasnat, M.; Shah, K.; Ansari, M. T. Design, Synthesis and Evaluation of DNA Nano-Cubes as a Core Material Protected by the Alginate Coating for Oral Administration of Anti-Diabetic Drug. *J. Food Drug Anal.* **2019**, *27*, 805–814.
16. Nadarajah, B.; Alifragis, P.; Wong, R. O. L.; Parnavelas, J. G. Neuronal Migration in the Developing Cerebral Cortex: Observations Based on Real-Time Imaging. *Cerebral Cortex*. **2003**, *13*, 607–611.
17. Afshan, N.; Ali, M.; Wang, M.; Baig, M. M. F. A.; Xiao, S. J. DNA Nanotubes Assembled from Tensegrity Triangle Tiles with Circular DNA Scaffolds. *Nanoscale* **2017**, *9*, 17181–17185.
18. Baig, M. M. F. A.; Naveed, M.; Abbas, M.; Chunxia, W.; Ullah, S.; Hasnat, M.; Shad, A.; Muhammad, S.; Jilany Khan, G.; Tayyab Ansari, M. DNA Scaffold Nanoparticles Coated with HPMC/EC for Oral Delivery. *Int. J. Pharm.* **2019**, *562*, 321–332.
19. Ali, M. M.; Li, F.; Zhang, Z.; Zhang, K.; Kang, D. K.; Ankrum, J. A.; Le, X. C.; Zhao, W. Rolling Circle Amplification: A Versatile Tool for Chemical Biology, Materials Science and Medicine. *Chem. Soc. Rev.* **2014**, *43*, 3324–3341.
20. Charrier, C.; MacHado, P.; Tweedie-Cullen, R. Y.; Rutishauser, D.; Mansuy, I. M.; Triller, A. A Crosstalk between B1 and B3 Integrins Controls Glycine Receptor and Gephyrin Trafficking at Synapses. *Nat. Neurosci.* **2010**, *13*, 1388–1395.
21. Hiesberger, T.; Trommsdorff, M.; Howell, B. W.; Goffinet, A.; Mumby, M. C.; Cooper, J. A.; Herz, J. Direct Binding of Reelin to VLDL Receptor and ApoE Receptor 2 Induces Tyrosine Phosphorylation of Disabled-1 and Modulates Tau Phosphorylation. *Neuron* **1999**, *24*, 481–489.
22. Song, L.; Falzone, N.; Vallis, K. A. EGF-Coated Gold Nanoparticles Provide an Efficient Nano-Scale Delivery System for the Molecular Radiotherapy of EGFR-Positive Cancer. *Int. J. Radiat. Biol.* **2016**, *92*, 716–723.
23. Paviolo, C.; Chon, J. W. M.; Clayton, A. H. A. Inhibiting EGFR Clustering and Cell Proliferation with Gold Nanoparticles. *Small* **2015**, *11*, 1638–1643.
24. Lozano-Torres, B.; Galiana, I.; Rovira, M.; Garrido, E.; Chaib, S.; Bernardos, A.; Muñoz-Espín, D.; Serrano, M.; Martínez-Máñez, R.; Sancenón, F. An OFF-ON Two-Photon Fluorescent Probe for Tracking Cell Senescence in Vivo. *J. Am. Chem. Soc.* **2017**, *139*, 8808–8811.
25. Berg, K.; Lange, T.; Mittelberger, F.; Schumacher, U.; Hahn, U. Selection and Characterization of an A6β4 Integrin Blocking DNA Aptamer. *Mol. Ther. Nucleic Acids* **2016**, *5*, e294.

DOI: 10.31635/ccschem.020.202000456
Citation: *CCS Chem.* **2020**, 2, 2381–2393
Citation denotes calendar and volume year of first online publication.
Issue Assignment: Volume 3 (2021), Issue 9

26. Dutta, P. K.; Zhang, Y.; Blanchard, A. T.; Ge, C.; Rushdi, M.; Weiss, K.; Zhu, C.; Ke, Y.; Salaita, K. Programmable Multivalent DNA-Origami Tension Probes for Reporting Cellular Traction Forces. *Nano Lett*. **2018**, *18*, 4803–4811.
27. Zhang, Y.; Ge, C.; Zhu, C.; Salaita, K. DNA-Based Digital Tension Probes Reveal Integrin Forces during Early Cell Adhesion. *Nat. Commun*. **2014**, *5*, 1–10.
28. Brockman, J. M.; Blanchard, A. T.; Pui-Yan, V.; Derricotte, W. D.; Zhang, Y.; Fay, M. E.; Lam, W. A.; Evangelista, F. A.; Mattheyses, A. L.; Salaita, K. Mapping the 3D Orientation of Piconewton Integrin Traction Forces. *Nat. Methods* **2018**, *15*, 115–118.
29. Deraedt, C.; Salmon, L.; Gatard, S.; Ciganda, R.; Hernandez, R.; Ruiz, J.; Astruc, D. Sodium Borohydride Stabilizes Very Active Gold Nanoparticle Catalysts. *Chem. Commun*. **2014**, *50*, 14194–14196.
30. Shen, B.; Linko, V.; Tapio, K.; Kostiainen, M. A.; Toppari, J. J. Custom-Shaped Metal Nanostructures Based on DNA Origami Silhouettes. *Nanoscale* **2015**, *7*, 11267–11272.
31. Baig, M. M. F. A.; Khan, S.; Naeem, M. A.; Khan, G. J.; Ansari, M. T. Vildagliptin Loaded Triangular DNA Nanospheres Coated with Eudragit for Oral Delivery and Better Glycemic Control in Type 2 Diabetes Mellitus. *Biomed. Pharmacother*. **2018**, *97*, 1250–1258.
32. Baig, M. M. F. A.; Lai, W. F.; Akhtar, M. F.; Saleem, A.; Mikrani, R.; Farooq, M. A.; Ahmed, S. A.; Tahir, A.; Naveed, M.; Abbas, M.; Ansari, M. T. Targeting Folate Receptors (A1) to Internalize the Bleomycin Loaded DNA-Nanotubes into Prostate Cancer Xenograft CWR22R Cells. *J. Mol. Liq*. **2020**, *316*, 113785.
33. Calatrava-Pérez, E.; Bright, S. A.; Achermann, S.; Moylan, C.; Senge, M. O.; Veale, E. B.; Williams, D. C.; Gunnlaugsson, T.; Scanlan, E. M. Glycosidase Activated Release of Fluorescent 1,8-Naphthalimide Probes for Tumor Cell Imaging from Glycosylated "pro-Probes." *Chem. Commun*. **2016**, *52*, 13086–13089.
34. Parak, W. J.; Pellegrino, T.; Micheel, C. M.; Gerion, D.; Williams, S. C.; Alivisatos, A. P. Conformation of Oligonucleotides Attached to Gold Nanocrystals Probed by Gel Electrophoresis. *Nano Lett*. **2003**, *3*, 33–36.
35. Baig, M. M. F. A.; Lai, W. F.; Ashraf, S.; Saleem, A.; Akhtar, M. F.; Mikrani, R.; Naveed, M.; Siddique, F.; Taleb, A.; Mudassir, J.; Khan, G. J.; Ansari, M. T. The Integrin Facilitated Internalization of Fibronectin-Functionalized Camptothecin-Loaded DNA-Nanofibers for High-Efficiency Anticancer Effects. *Drug Deliv. Transl. Res*. **2020**, *10*, 1381–1392.
36. Liu, H.; Dolkas, J.; Hoang, K.; Angert, M.; Chernov, A. V.; Remacle, A. G.; Shiryaev, S. A.; Strongin, A. Y.; Nishihara, T.; Shubayev, V. I. The Alternatively Spliced Fibronectin CS1 Isoform Regulates IL-17A Levels and Mechanical Allodynia after Peripheral Nerve Injury. *J. Neuroinflamm*. **2015**, *12*, 158.
37. Liu, W. Q.; Martinez, J. A.; Durand, J.; Wildering, W.; Zochodne, D. W. RGD-Mediated Adhesive Interactions Are Important for Peripheral Axon Outgrowth in Vivo. *Neurobiol. Dis*. **2009**, *34*, 11–22.
38. Zhao, S.; Fan, W.; Guo, X.; Xue, L.; Berninger, B.; Salierno, M. J.; del Campo, A. Microenvironments to Study Migration and Somal Translocation in Cortical Neurons. *Biomaterials* **2018**, *156*, 238–247.
39. Bernal, J. Thyroid Hormone Regulated Genes in Cerebral Cortex Development. *J. Endocrinol*. **2017**, *232*, R83–R97.
40. Liu, Y.; Galior, K.; Ma, V. P. Y.; Salaita, K. Molecular Tension Probes for Imaging Forces at the Cell Surface. *Acc. Chem. Res*. **2017**, *50*, 2915–2924.
41. Cooper, J.; Giancotti, F. G. Integrin Signaling in Cancer: Mechanotransduction, Stemness, Epithelial Plasticity, and Therapeutic Resistance. *Cancer Cell*. **2019**, *35*, 347–367.
42. Blakely, B. L.; Dumelin, C. E.; Trappmann, B.; McGregor, L. M.; Choi, C. K.; Anthony, P. C.; Duesterberg, V. K.; Baker, B. M.; Block, S. M.; Liu, D. R.; Chen, C. S. A DNA-Based Molecular Probe for Optically Reporting Cellular Traction Forces. *Nat. Methods* **2014**, *11*, 1229–1232.
43. Liu, Q.; Jin, L. H. Organ-to-Organ Communication: A Drosophila Gastrointestinal Tract Perspective. *Front. Cell Dev. Biol*. **2017**, *5*, 40.
44. Zhang, Y.; Qiu, Y.; Blanchard, A. T.; Chang, Y.; Brockman, J. M.; Ma, V. P.-Y.; Lam, W. A.; Salaita, K. Platelet Integrins Exhibit Anisotropic Mechanosensing and Harness Piconewton Forces to Mediate Platelet Aggregation. *Proc. Natl. Acad. Sci. U. S. A.* **2018**, *115*, 325–330.
45. Hoe, H.; Lee, K. J.; Carney, R. S. E.; Lee, J.; Lee, J.; Howell, B. W.; Hyman, B. T.; Pak, D. T. S.; Rebeck, G. W. Interaction of Reelin with APP Promotes Neurite Outgrowth. *J. Neurosci*. **2009**, *29*, 7459–7473.
46. Lee, G. H.; D'Arcangelo, G. New Insights into Reelin-Mediated Signaling Pathways. *Front. Cell. Neurosci*. **2016**, *10*, 122.
47. Ernfors, P.; Hallbook, F.; Ebendal, T.; Shooter, E. M.; Radeke, M. J.; Misko, T. P.; Persson, H. Developmental and Regional Expression of β-Nerve Growth Factor Receptor MRNA in the Chick and Rat. *Neuron* **1988**, *1*, 983–996.
48. Nguyen, L.; Hippenmeyer, S. Cellular and Molecular Control of Neuronal Migration. *Adv. Exper. Med. Biol.*. **2014**, *800*, 97–111.
49. Polackwich, R. J.; Koch, D.; McAllister, R.; Geller, H. M.; Urbach, J. S. Traction Force and Tension Fluctuations in Growing Axons. *Front. Cell. Neurosci*. **2015**, *9*, 417.
50. Athamneh, A. I. M.; Suter, D. M. Quantifying Mechanical Force in Axonal Growth and Guidance. *Front. Cell. Neurosci*. **2015**, *9*, 359.
51. Cheah, M.; Andrews, M. Integrin Activation: Implications for Axon Regeneration. *Cells* **2018**, *7*, 20.
52. Soba, P.; Han, C.; Zheng, Y.; Perea, D.; Miguel-Aliaga, I.; Jan, L. Y.; Jan, Y. N. The Ret Receptor Regulates Sensory Neuron Dendrite Growth and Integrin Mediated Adhesion. *Elife* **2015**, *4*, e05491.
53. Jiang, J.; Zhang, Z. H.; Yuan, X. B.; Poo, M. M. Spatiotemporal Dynamics of Traction Forces Show Three Contraction Centers in Migratory Neurons. *J. Cell Biol.* **2015**, *209*, 759–774.
54. Grabham, P. W.; Goldberg, D. J. Nerve Growth Factor Stimulates the Accumulation of B1 Integrin at the Tips of Filopodia in the Growth Cones of Sympathetic Neurons. *J. Neurosci*. **2018**, *17*, 5455–5465.

DOI: 10.31635/ccschem.020.202000456
Citation: *CCS Chem.* **2020**, 2, 2381–2393
Citation denotes calendar and volume year of first online publication.
Issue Assignment: Volume 3 (2021), Issue 9